

## Precision Shock Tuning on the National Ignition Facility

H. F. Robey,<sup>1</sup> P. M. Celliers,<sup>1</sup> J. L. Kline,<sup>2</sup> A. J. Mackinnon,<sup>1</sup> T. R. Boehly,<sup>3</sup> O. L. Landen,<sup>1</sup> J. H. Eggert,<sup>1</sup> D. Hicks,<sup>1</sup> S. Le Pape,<sup>1</sup> D. R. Farley,<sup>1</sup> M. W. Bowers,<sup>1</sup> K. G. Krauter,<sup>1</sup> D. H. Munro,<sup>1</sup> O. S. Jones,<sup>1</sup> J. L. Milovich,<sup>1</sup> D. Clark,<sup>1</sup> B. K. Spears,<sup>1</sup> R. P. J. Town,<sup>1</sup> S. W. Haan,<sup>1</sup> S. Dixit,<sup>1</sup> M. B. Schneider,<sup>1</sup> E. L. Dewald,<sup>1</sup> K. Widmann,<sup>1</sup> J. D. Moody,<sup>1</sup> T. D. Döppner,<sup>1</sup> H. B. Radousky,<sup>1</sup> A. Nikroo,<sup>4</sup> J. J. Kroll,<sup>1</sup> A. V. Hamza,<sup>1</sup> J. B. Horner,<sup>1</sup> S. D. Bhandarkar,<sup>1</sup> E. Dzenitis,<sup>1</sup> E. Alger,<sup>4</sup> E. Giraldez,<sup>4</sup> C. Castro,<sup>1</sup> K. Moreno,<sup>4</sup> C. Haynam,<sup>1</sup> K. N. LaFortune,<sup>1</sup> C. Widmayer,<sup>1</sup> M. Shaw,<sup>1</sup> K. Jancaitis,<sup>1</sup> T. Parham,<sup>1</sup> D. M. Holunga,<sup>1</sup> C. F. Walters,<sup>1</sup> B. Haid,<sup>1</sup> T. Malsbury,<sup>1</sup> D. Trummer,<sup>1</sup> K. R. Coffee,<sup>1</sup> B. Burr,<sup>1</sup> L. V. Berzins,<sup>1</sup> C. Choate,<sup>1</sup> S. J. Brereton,<sup>1</sup> S. Azevedo,<sup>1</sup> H. Chandrasekaran,<sup>1</sup> S. Glenzer,<sup>1</sup> J. A. Caggiano,<sup>1</sup> J. P. Knauer,<sup>3</sup> J. A. Frenje,<sup>5</sup> D. T. Casey,<sup>5</sup> M. Gatu Johnson,<sup>5</sup> F. H. Séguin,<sup>5</sup> B. K. Young,<sup>1</sup> M. J. Edwards,<sup>1</sup> B. M. Van Wonterghem,<sup>1</sup> J. Kilkenny,<sup>1</sup> B. J. MacGowan,<sup>1</sup> J. Atherton,<sup>1</sup> J. D. Lindl,<sup>1</sup> D. D. Meyerhofer,<sup>3</sup> and E. Moses<sup>1</sup>

<sup>1</sup>Lawrence Livermore National Laboratory, Livermore, California 94551, USA

<sup>2</sup>Los Alamos National Laboratory, Los Alamos, New Mexico 87545, USA

<sup>3</sup>Laboratory for Laser Energetics, Rochester, New York 14623, USA

<sup>4</sup>General Atomics, San Diego, California 92186, USA

<sup>5</sup>Massachusetts Institute of Technology, Cambridge, Massachusetts 02139, USA

(Received 8 October 2011; published 24 May 2012)

Ignition implosions on the National Ignition Facility [J. D. Lindl *et al.*, *Phys. Plasmas* **11**, 339 (2004)] are underway with the goal of compressing deuterium-tritium fuel to a sufficiently high areal density ( $\rho R$ ) to sustain a self-propagating burn wave required for fusion power gain greater than unity. These implosions are driven with a very carefully tailored sequence of four shock waves that must be timed to very high precision to keep the fuel entropy and adiabat low and  $\rho R$  high. The first series of precision tuning experiments on the National Ignition Facility, which use optical diagnostics to directly measure the strength and timing of all four shocks inside a hohlraum-driven, cryogenic liquid-deuterium-filled capsule interior have now been performed. The results of these experiments are presented demonstrating a significant decrease in adiabat over previously untuned implosions. The impact of the improved shock timing is confirmed in related deuterium-tritium layered capsule implosions, which show the highest fuel compression ( $\rho R \sim 1.0$  g/cm<sup>2</sup>) measured to date, exceeding the previous record [V. Goncharov *et al.*, *Phys. Rev. Lett.* **104**, 165001 (2010)] by more than a factor of 3. The experiments also clearly reveal an issue with the 4th shock velocity, which is observed to be 20% slower than predictions from numerical simulation.

DOI: 10.1103/PhysRevLett.108.215004

PACS numbers: 52.57.-z, 43.25.Cb, 43.40.Jc

Capsule implosions on the National Ignition Facility (NIF) [1] are underway using the indirect-drive concept, where the energy of a temporally shaped laser pulse is converted into thermal x rays in a cylindrical high-Z enclosure (hohlraum). This x-ray radiation ablates the surface of a low-Z spherical shell, which surrounds a cryogenic layer of deuterium-tritium (DT) fuel, imploding the fuel to create the high density and temperature plasma conditions required to initiate DT fusion reactions in the central hot spot core. Achieving ignition requires the assembly of a fuel layer with sufficient areal or column density ( $\rho R$ ) to inertially confine the burning fuel for a sufficient duration to sustain a self-propagating burn wave required for fusion power gain greater than unity. To date, the highest value of  $\rho R$  reported (0.3 g/cm<sup>2</sup>) has been inferred from direct-drive experiments [2] on the OMEGA Laser Facility [3] at the University of Rochester. The increased scale and highly accurate and repeatable laser pulse shaping capabilities of the NIF enable ignition experiments that can compress the fuel to significantly higher densities ultimately reaching

the requirement for ignition on NIF of a minimum  $\rho R \approx 1.3$  g/cm<sup>2</sup> [4,5].

To achieve high  $\rho R$ , a series of tuning experiments [6] are being conducted to optimize the laser coupling to the hohlraum [7,8], the implosion symmetry [9,10], and the strength and timing of the multiple shock waves used to compress and accelerate the fuel layer while maintaining a low adiabat. The adiabat (directly related to the entropy) is defined as the ratio of the mass-averaged fuel pressure to the Fermi degenerate pressure [4]. High fuel  $\rho R$  requires that the fuel remain highly compressible with an adiabat goal [4] of  $1.47 \pm 0.1$ . Early NIF implosions using untuned laser pulses demonstrated an adiabat of  $1.9 \pm 0.2$  [11]. This Letter reports the results from the first precision shock tuning series on NIF, which has resulted in a decreased implosion adiabat of  $1.5 \pm 0.1$ .

The target geometry used for shock tuning experiments, a diagnostic variation of the NIF ignition hohlraum (10.01 mm  $\times$  5.44 mm diameter Au cylinder), is shown in the inset of Fig. 1. The target is identical to the NIF

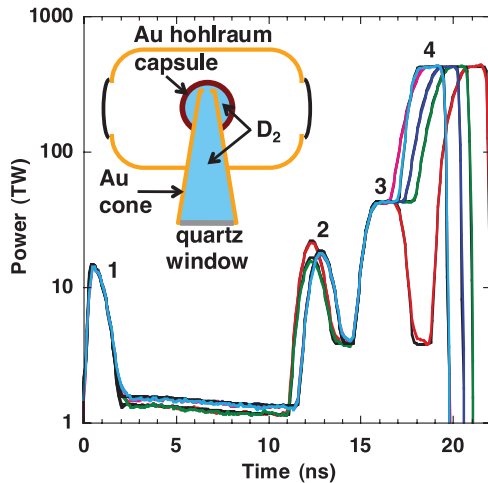


FIG. 1 (color). NIF laser power history for the tuning series. Shot N110513 (red), N110515 (green), N110517 (blue), N110521 (magenta), and N110526 (cyan). Inset shows the hohlraum geometry for these experiments.

ignition hohlraum with the exception of a Au reentrant cone that enters through the hohlraum wall into the interior of a Ge-doped polystyrene (CH) capsule ( $r = 1108 \mu\text{m}$ , thickness =  $190 \mu\text{m}$ ) providing optical access to the propagating shocks as they sequentially overtake preceding shocks. The volume inside both the capsule and Au cone is filled with liquid deuterium (21.5 K), which provides an excellent surrogate to the shock propagation in the DT ice layer present in ignition targets.

The shocks are generated by a very precise laser-driven power history ( $0.35 \mu\text{m}$  wavelength) that consists of a series of 4 pulses of increasing power. Figure 1 shows the laser pulses used for the five shots in the present tuning series. The requested pulse shape, shown in black, can only be distinguished from the delivered pulse at the low-power levels following the 1st, 2nd, and 3rd pulses. For all shots, the full 192 beams of NIF were fired delivering a total energy of 0.988–1.04 MJ, within 1% of the request. Peak laser power was 420 TW for all shots in this series.

The laser pulse shape for the initial shots employed an added delay between the 2nd, 3rd, and 4th pulses in order to provide sufficient duration of each shock for accurate measurement. The 4th pulse was truncated in duration compared to the point design ignition pulse (1.3 MJ), as the shock timing at the measurement location ( $r = 720\text{--}918 \mu\text{m}$ , inside the capsule) is completely determined by the time at which the laser pulse first reaches peak power.

Diagnostic techniques have been developed and tested [12] on OMEGA to diagnose the strength and absolute timing of shocks in a liquid-deuterium ( $\text{D}_2$ ) filled capsule interior to very high accuracy. These techniques have been demonstrated on both directly-driven capsule implosions on OMEGA [13] and indirectly-driven, hohlraum targets on NIF [11]. The NIF targets are specifically modified to

withstand the 2 order-of-magnitude increase in laser fluence over that employed in the OMEGA experiments.

The diagnostic technique employs the velocity interferometer system for any reflector (VISAR) [14,15], where the reflector in this case is the leading shock front in the liquid  $\text{D}_2$  surrogate fuel, which has high reflectivity to the 660 nm VISAR laser. VISAR measures the strength (velocity) of the shocks to an accuracy of  $<1 \mu\text{m}/\text{ns}$ . The leading shock velocity following successive shock mergers is nominally 20, 35, 70, and  $115 \mu\text{m}/\text{ns}$  in the current point design, corresponding to pressures in the surrogate  $\text{D}_2$  fuel of 0.6, 2.3, 8.7, and 26.5 MBar. The relative timing of these shocks is observed by recording the time at which subsequent shocks overtake preceding shocks. This is indicated by a clearly observed discontinuity in the VISAR data, and is measured to an accuracy of 50 ps. Integrating the VISAR velocity history, the radial location of these shock mergers is obtained to an accuracy of  $<1 \mu\text{m}$ .

Figure 2 shows VISAR streaked interferometer images for three of the shots. Time runs from left to right, and lateral (bottom-to-top) motion of the interference fringes is directly proportional to the shock velocity, with fringe motion upward indicating an accelerating shock. The relatively darker fringes at the top and bottom of each image are reflections of the VISAR laser from a stationary Au aperture at the tip of the VISAR viewing cone as seen in the inset of Fig. 1. Fringe motion between these stationary references is due to reflections from the leading shock front in liquid  $\text{D}_2$ . Discontinuities in the fringe positions

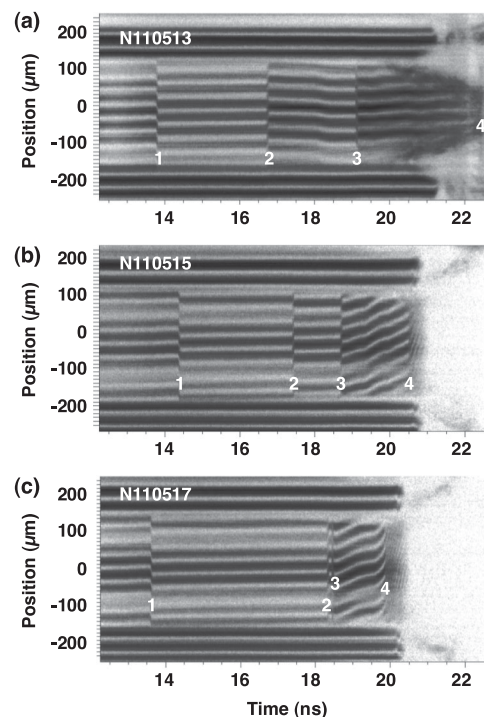


FIG. 2. VISAR streak images of three sequential tuning shots. Arrival time of each of the four shocks in liquid  $\text{D}_2$  is indicated.

clearly indicate the arrival time of shocks. The first of these, labeled “1” and seen near 14 ns, is the time at which the 1st shock breaks out of the Ge-doped CH ablator into the liquid  $D_2$ . Subsequent discontinuities indicate the time at which the increasingly stronger 2nd, 3rd, and 4th shocks overtake or merge with preceding shocks. As is seen in Fig. 2, the interval between successive mergers is initially several ns but is systematically decreased in subsequent shots to approach the goal of having the first three shocks merge at a single time [18.5 ns in Fig. 2(c)] and correspondingly a single radial location inside the capsule.

The pulse shape changes required to tune the shocks are specified by preshot calculated “playbooks”, which are obtained from 2D integrated-hohlraum simulations (HYDRA [16]) that predict the expected changes in all shock velocities, accelerations, merger times, and radii as a function of the power and time of each epoch of the laser pulse shape (initial picket, low-power trough, 2nd, 3rd, and 4th pulses). Figure 3 shows a comparison of the measured data with several of the playbook predictions. Figure 3(a), for example, compares the time of 1st shock breakout from the CH ablator into the  $D_2$  fuel as a function of the laser energy in the initial picket (0–2 ns). The measured slope is within 30% of the predicted slope. The picket energy variation reported in Fig. 3(a) is limited in both duration (0–2 ns) as well as spatial location within the hohlraum (top half in Fig. 1 inset, where the VISAR measurement is made).

The nominal picket energy is approximately 15 kJ, so an 8% variation is 1.2 kJ, which is  $\sim 0.1\%$  of the total pulse energy. The ignition requirement for picket energy is  $\pm 5\%$ , and Fig. 3(a) illustrates the effect of this variation on the shock timing. Shot-to-shot variation in picket energy has subsequently been improved by more frequent inspection of debris accumulation on the optics (further details are given in [17]).

Figure 3(b) shows a similar comparison for the 2nd shock velocity, which depends almost exclusively on the 2nd pulse laser power. The first shot showed a velocity of  $36.5 \mu\text{m/ns}$ , slightly higher than the goal of  $33.7 \pm 1.7 \mu\text{m/ns}$ . The second shot reduced the 2nd pulse laser power by 24% and overcorrected the velocity to  $29.7 \mu\text{m/ns}$ . The laser power was increased and held constant for the last three shots, which show a shot-to-shot variability of  $\pm 1.05 \mu\text{m/ns}$  ( $\pm 3\%$  of the 3-shot average). This illustrates the level of shot-to-shot repeatability on NIF.

Shock merger locations were found to follow preshot predictions very well as indicated by the example of the shock 3–4 merger depth (radial distance into the  $D_2$  from the inner surface of the ablator) vs the launch time of the 4th pulse. A similar level of agreement was found for all other shock merger depths.

By contrast with the other measurements, the 4th shock velocity was not observed to be in agreement with

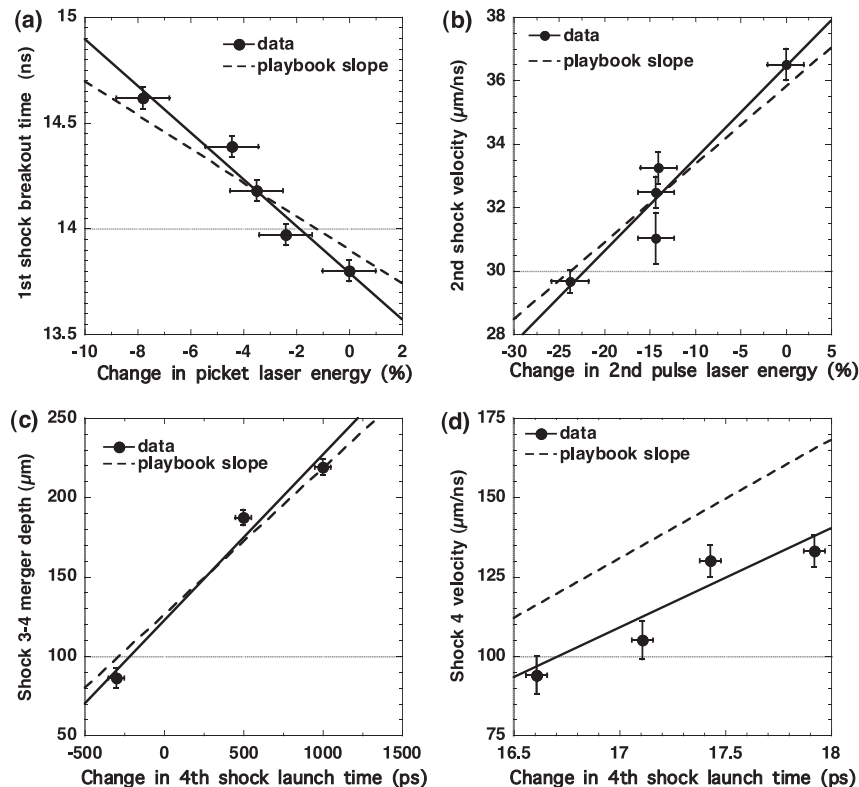


FIG. 3. Comparison of measured vs predicted tuning sensitivities. (a) time of 1st shock breakout into liquid  $D_2$ , (b) 2nd shock velocity, (c) depth of shock 3–4 merger, (d) 4th shock velocity.

predictions as shown in Fig. 3(d). The 4th shock velocity is plotted as a function of the 4th pulse launch time. Since the 4th shock is strongly accelerating, the measured velocity (initially observed upon merger with the 3rd shock) increases with delay time as expected with a slope within 16% of the playbook. The magnitude of the 4th shock velocity, however, is lower than the simulations by 20–25  $\mu\text{m}/\text{ns}$  ( $\sim 20\%$ ). The 4th shock velocity is measured in these experiments at a radius  $r > 700 \mu\text{m}$  as compared to the ablator shell velocity measurements of [18], where a backlit x-ray radiograph of an imploding capsule also measured velocities approximately 15% lower than simulations, but in those experiments the velocity was measured at much smaller radii (200–400  $\mu\text{m}$ ). This suggests that the lack of agreement between data and simulations originates early in the 4th pulse rather than later in the implosion. The margin for successful ignition scales with  $v_{\text{fuel}}^8$  [4]. This observed velocity deficit is therefore a serious degradation to the implosion performance. Possible sources of this discrepancy include uncertainties in the laser coupling to the hohlraum, x-ray absorption in the ablator, and equation of state of the ablator. These are currently the focus of ongoing investigation.

Figure 4 shows a comparison of the measured VISAR velocity histories with those from postshot simulations. The VISAR velocity data are shown with the black curves, and the postshot 2D HYDRA simulations including the measured laser power, measured capsule and hohlraum dimensions, and measured laser backscatter are shown with the red curves. The simulations also account for measured spatial laser power imbalance and account for the effect of cross-beam power transfer between inner and

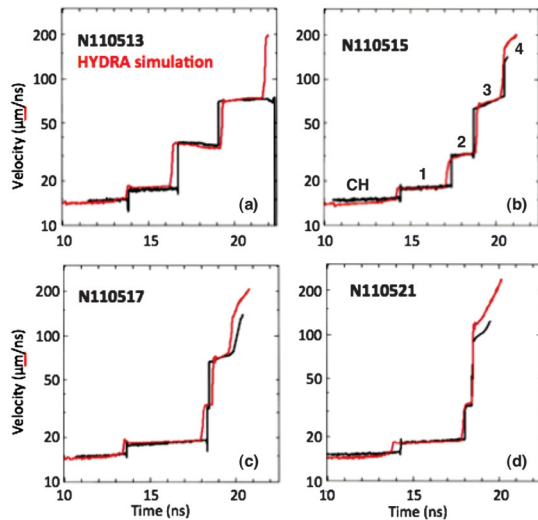


FIG. 4 (color). (a) Shock velocity history for four shots in the tuning series. Black curve is VISAR data. Red curve is simulated VISAR from 2D integrated-hohlraum simulations. The individual shocks are labeled in (b).

outer cones, which has been found to play a considerable role throughout the laser pulse [19].

Figure 4(a) shows the velocity history for an initially untuned pulse with the 3rd and 4th laser pulses delayed by 1 ns each. Figs. 4(b)–4(d) show the corresponding velocity histories as the laser pulse is adjusted to achieve a coalescence of the first three shocks at the proper depth from the inner surface of the ablator (81  $\mu\text{m}$ ). The results are qualitatively similar to those presented in [13] for direct-drive conditions. A few differences are noted, however. Because of the substantially thicker ablator of NIF capsules (190  $\mu\text{m}$ ) vs OMEGA capsules (10  $\mu\text{m}$ ) and the reduced  $M$ -band flux measured in NIF hohlraums, the VISAR is now able to diagnose the shock velocity inside the CH(Ge) ablator as well as in the  $\text{D}_2$ . The closer proximity of the liquid  $\text{D}_2$  to the ablation front in OMEGA implosions precludes this observation due to photoionization of the CH [13]. The shock levels are also observed to be much more constant in velocity than in [13]. This is a consequence of the precision pulse shaping capabilities of NIF with the very low, but nonzero, trough power levels following the initial two picket features (Fig. 1) and the very high contrast ratio (max-to-min power ratio  $>400$ ) achievable on NIF. This allows sequential shocks to compress the fuel layer without suffering a decompression that results from decaying, unsupported shock velocities. The agreement between data and 2D simulations in Fig. 4 is quite good, with the important exception of the 4th shock velocity as discussed earlier.

Figure 5 shows the measured shock trajectories in the liquid  $\text{D}_2$  with  $r = 0$  being the ablator- $\text{D}_2$  interface. The positions of the mergers between shocks are indicated with the symbols. The point design goal is to have the merger of shocks 1–2 and 2–3 positioned at 81  $\mu\text{m}$ , which, accounting for the small difference in sound speeds between  $\text{D}_2$  and DT, would put this triple-shock coalescence at a depth

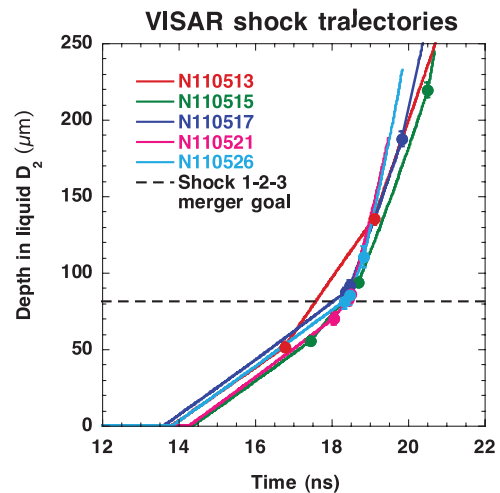


FIG. 5 (color). Shock trajectories ( $r, t$ ) in liquid  $\text{D}_2$  for the 5 shot tuning series.



5  $\mu\text{m}$  greater than the thickness of a DT ice layer in an ignition target [4]. The goal for the shock 3–4 merger is slightly deeper at 97  $\mu\text{m}$ . In the early shots, the merger positions were many tens of microns away from this goal, but as the tuning progressed, the merger positions were adjusted to the goal with high precision and acceptable repeatability.

The fuel entropy and adiabat are not measured directly in these experiments. We estimate the adiabat for an equivalent DT layered implosion using the procedure outline in [11]. To summarize: a radiation drive source in 1D simulations of the shock timing shots is adjusted to produce a VISAR velocity history that matches the data to within the experimental error bars. The peak of the drive, beyond that measurable by VISAR, is constrained by matching the bang time to that measured in a corresponding layered target implosion. The resulting drive from this procedure is then applied to the as-shot conditions of related DT ignition shots giving an adiabat of  $1.41 \pm 0.05$  from the 1D (spherical) simulations and  $1.5 \pm 0.1$  from the 2D simulations that include the effects of low-mode asymmetry as well.

An independent confirmation of the improvement in adiabat due to shock tuning is obtained by companion shots employing DT ice fuel layers [20], which were subsequently shot using the tuned shock timing from the present measurements. In these experiments, the fuel compression is inferred by direct measurement of the ratio of the down-scattered neutron fraction in the 10–12 MeV range over the unscattered fraction measured from 13–15 MeV. This down-scattered ratio is directly proportional to the fuel areal density,  $\rho R$ . A more detailed discussion of the full suite of neutron diagnostics employed on NIF is given in [20]. Previous untuned shots gave a measured  $\rho R$  of 0.55 g/cm<sup>2</sup>. Following the present tuning series, four layered capsule implosions using the tuned laser pulse gave  $\rho R$  measurements of 0.89, 0.90, 0.73, and 0.92 g/cm<sup>2</sup>, nearly a factor of 2 improvement over untuned NIF shots, and approximately a factor of 3 increase over the highest reported measurement in direct drive. Future efforts will be directed toward an understanding of the observed velocity

discrepancy in the final shock and capsule velocities. Resolving this discrepancy should result in a further increase in  $\rho R$ , putting the implosions even closer to the desired ignition regime.

This work was performed under the auspices of the Lawrence Livermore National Security, LLC, (LLNS) under Contract No. DE-AC52-07NA27344.

- 
- [1] J. D. Lindl, P. Amendt, R. L. Berger, S. G. Glendinning, S. H. Glenzer, S. W. Haan, R. L. Kauffman, O. L. Landen, and L. J. Suter, *Phys. Plasmas* **11**, 339 (2004).
  - [2] V. Goncharov *et al.*, *Phys. Rev. Lett.* **104**, 165001 (2010).
  - [3] T. R. Boehly *et al.*, *Opt. Commun.* **133**, 495 (1997).
  - [4] S. W. Haan *et al.*, *Phys. Plasmas* **18**, 051001 (2011).
  - [5] M. J. Edwards *et al.*, *Phys. Plasmas* **18**, 051003 (2011).
  - [6] O. Landen *et al.*, *Phys. Plasmas* **18**, 051002 (2011).
  - [7] J. L. Kline *et al.*, *Phys. Rev. Lett.* **106**, 085003 (2011).
  - [8] N. Meezan *et al.*, *Phys. Plasmas* **17**, 056304 (2010).
  - [9] P. Michel *et al.*, *Phys. Rev. Lett.* **102**, 025004 (2009).
  - [10] G. Kyrala *et al.*, *Phys. Plasmas* **18**, 056307 (2011).
  - [11] H. F. Robey *et al.*, *Phys. Plasmas* **19**, 042706 (2012).
  - [12] T. R. Boehly *et al.*, *Phys. Plasmas* **16**, 056302 (2009).
  - [13] T. R. Boehly, V. N. Goncharov, W. Seka, M. A. Barrios, P. M. Celliers, D. G. Hicks, G. W. Collins, S. X. Hu, J. A. Marozas, and D. D. Meyerhofer, *Phys. Rev. Lett.* **106**, 195005 (2011).
  - [14] L. M. Barker and R. E. Hollenbach, *J. Appl. Phys.* **43**, 4669 (1972).
  - [15] P. M. Celliers, D. K. Bradley, G. W. Collins, D. G. Hicks, T. R. Boehly, and W. J. Armstrong, *Rev. Sci. Instrum.* **75**, 4916 (2004).
  - [16] M. M. Marinak, G. D. Kerbel, N. A. Gentile, O. Jones, D. Munro, S. Pollaine, T. R. Dittrich, and S. W. Haan, *Phys. Plasmas* **8**, 2275 (2001).
  - [17] H. F. Robey *et al.*, *Phys. Plasmas* (to be published).
  - [18] D. G. Hicks, B. K. Spears, D. G. Braun, R. E. Olson, C. M. Sorce, P. M. Celliers, G. W. Collins, and O. L. Landen, *Phys. Plasmas* **17**, 102703 (2010).
  - [19] P. Michel *et al.*, *Phys. Plasmas* **17**, 056305 (2010).
  - [20] A. J. Mackinnon *et al.*, following Letter, *Phys. Rev. Lett.* **108**, 215005 (2012).